Synthesis and thermoelectric properties of $Bi_{2.5}Ca_{2.5}Co_2O_x$ layered cobaltites

Emmanuel Guilmeau
National Institute of Advanced Industrial Science and Technology, Osaka 563-8577, Japan

Masashi Mikami and Ryoji Funahashi[a)]
National Institute of Advanced Industrial Science and Technology, Midorigaoka, Ikeda, Osaka 563-8577, Japan; and CREST, Japan Science and Technology Agency, Ikeda, Osaka 563-8577, Japan

Daniel Chateigner
CRISMAT-ENSICAEN Laboratory, UMR CNRS 6508, 14050 Caen Cedex, France

(Received 12 October 2004; accepted 19 January 2005)

Bi–Ca–Co–O polycrystalline materials with a layered structure were prepared. The synthesis of the sintered specimens from two starting compositions, $Bi_{1.8}Ca_2Co_2O_x$ and $Bi_{2.5}Ca_{2.5}Co_2O_x$, revealed the latter is preferentially formed at high temperature (850 °C). The increase in sintering time was shown by growth of large platelike grains (up to 50 μm in diameter and several micrometers in thickness). The reaction mechanisms during the heat treatment and the preferential formation of the $Bi_{2.5}Ca_{2.5}Co_2O_x$ phase were observed by x-ray diffraction, thermogravimetry–differential thermal analysis, and scanning electron microscopy. These techniques supposed the presence of a liquid phase at high temperature, origin of a highly kinetic phase formation, and the growth of large grains. Interestingly the liquid phase reaction promotes an efficient stacking and sliding of grains during hot-forging treatment, and highly (00*l*) oriented materials were prepared. A relationship between thermoelectric performance, texture strength, and microstructure is clarified.

I. INTRODUCTION

Thermoelectric (TE) power generation is expected to provide a new energy source in the next few decades. Although intermetallic compounds, such as Bi_2Te_3 or PbTe, are actually used efficiently for practical applications, their technological scope is limited to low temperatures because of their low chemical stability at high temperatures. In contrast, new misfit-layered cobaltites, such as $NaCo_2O_4$,[1] $Ca_3Co_4O_9$,[2–4] or $Bi_2Sr_2Co_2O_x$,[5] have attracted much attention in the last seven years due to their promising TE properties and high melting or decomposition temperatures. These systems have been deeply studied in terms that Seebeck coefficient (*S*), electrical resistivity (ρ), and thermal conductivity (κ) were almost independent of one another due to deviation of the conventional band picture, indicating that each parameter can be independently controlled for improvement of TE properties. In addition to these well-known cobaltites, the high potential of the Bi–Ca–Co–O system[6,7] for practical applications has recently been highlighted. Maignan et al.[6] reported sintered specimens with large *S* values of ~140 μV/K, low electrical resistivity (ρ values of 40–60 mΩcm), and small κ of ~1 W/mK at 300 K. Itahara et al.[7] investigated texturing of bulk materials and succeeded in reducing ρ values to 20 mΩcm, thus leading to figure of merit values close to 0.13 at 1060 K. In this study, the Bi–Ca–Co–O system was investigated to elucidate its phase stability and to improve the TE performances of textured ceramics prepared by the hot-forging technique. We demonstrate the influence of starting material composition and process parameters on the phase formation and microstructure aspects (i.e., grain size) and discuss the TE properties of textured materials.

II. EXPERIMENTAL

The synthesis of the different samples was carried out in several steps. First, polycrystalline samples were prepared by solid-state reaction with Bi_2O_3, $CaCO_3$, and Co_3O_4 powders as starting materials. These powders were mixed by ball-milling in the compositions $Bi_{1.8}Ca_2Co_2O_x$ and $Bi_{2.5}Ca_{2.5}Co_2O_x$. Both powder mixtures were then made into pellets and sintered in air at 850 °C for 12 h, 25 h or 50 h.

Pellets of the $Bi_{2.5}Ca_{2.5}Co_2O_x$ composition sintered for 12, 25, or 50 h were manually ground and sieved (80-μm pore size). The resulting powders were variously

[a)]Address all correspondence to this author.
e-mail: funahashi-r@aist.go.jp
DOI: 10.1557/JMR.2005.0131

cold-pressed under uniaxial pressure of 120 MPa into 5 × 5 mm pellets with a thickness of 2 mm. The pellets were then placed in a hot-forging furnace between two 0.06-mm-thick gold sheets to avoid any reaction with the alumina square supports. The uniaxial pressure used during heating was 6 MPa, and the operating temperature was fixed at 850 °C for 20 h.

The microstructure of the sintered specimens was observed by scanning electron microscopy (SEM). Energy dispersive spectroscopy (EDS) was used to determine the cationic composition of the grains. X-ray diffraction (XRD) measurement was routinely used to check the phase formation and the presence of secondary phases. Quantitative texture analysis was performed on a Philips X'Pert 4-circle goniometer in the Bragg-Brentano geometry. Since our hot-forged materials have axially symmetric fiber textures (i.e., random in-plane distribution of crystallite *a* and *b* axes), the complete texture analysis was made by measuring the inclination of the {00*l*} crystallographic planes in terms of the sample surface.[8,9] The Gaussian integrated (005) peak intensities were normalized into distribution densities by the direct normalization procedure[9] and used as input to reconstruct χ-scans, which represent the {00*l*} plane dispersions of the crystallites. The maximum of the distribution densities (DD_{max}) was extracted from the χ-scan Gaussian profile and used as parameter for a quantitative appreciation of the crystallite dispersion and texture strength.[9] Thermogravimetry and differential thermal analysis (TG/DTA) were carried out on a Rigaku TG8120. The heating rate of the samples was 10 °C/min. The ρ values were measured along the *ab* plane direction, i.e., perpendicular to the fiber texture direction, using a conventional four-probe direct-current (dc) technique from room temperature to 1100 K in air. *S* values were calculated from a plot of TE voltage against temperature differential as measured in the 373–1073 K range in air using an instrument designed in our laboratory.[10] The textured specimens were cut into rectangular bars (3 × 0.3 × 10 mm) for measurement of transport properties.

III. RESULTS AND DISCUSSION

Figures 1 and 2 show the microstructure of pellets prepared from starting compositions of $Bi_{1.8}Ca_2Co_2O_x$ and $Bi_{2.5}Ca_{2.5}Co_2O_x$, respectively, and variously sintered at 850 °C for (a) 12 h, (b) 25 h, and (c, d) 50 h. Several interesting points should be noted. First, it appears clear that longer sintering dwell times induce larger platelike grains for both compositions. It should also be noted here that the grain size saturates with longer sintering times (over 50 h). In Figs. 1(d) and 2(d), the layered structure of the grains is clearly observable by many stacked layers along the thickness direction, which constitutes the *c* axis in the theoretical structure. On the other hand, it may be noted that the $Bi_{2.5}Ca_{2.5}Co_2O_x$ starting composition also promotes the growth of larger platelike grains, ~50 μm in diameter and ~8 μm in thickness, after 50 h of sintering. The improved grain growth for this composition can be

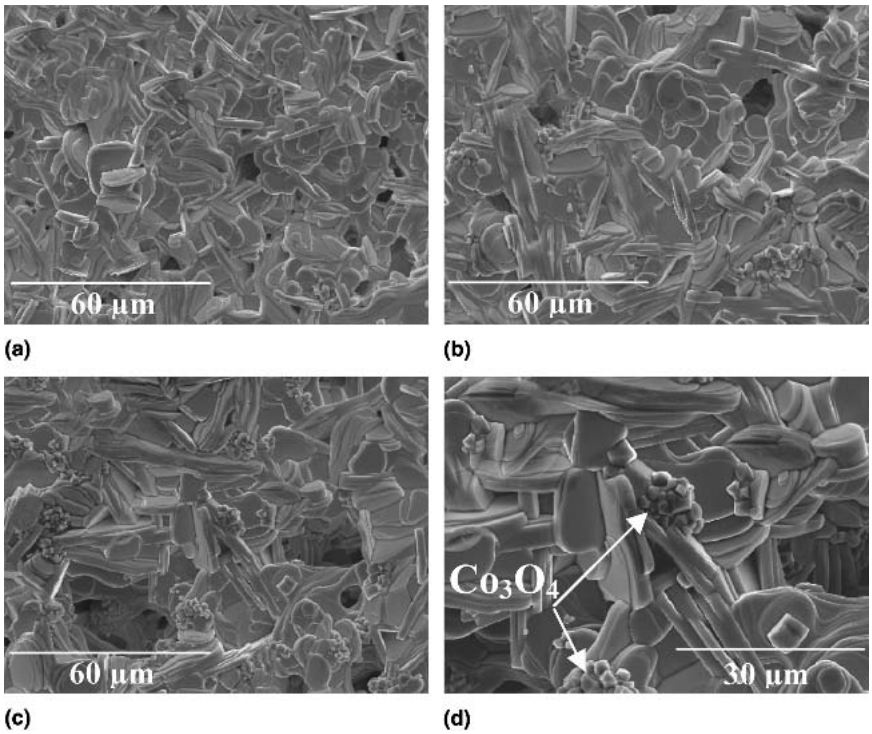

FIG. 1. SEM micrographs of pellets sintered for (a) 12 h, (b) 25 h, and (c, d) 50 h; $Bi_{1.8}Ca_2Co_2O_x$ starting composition.

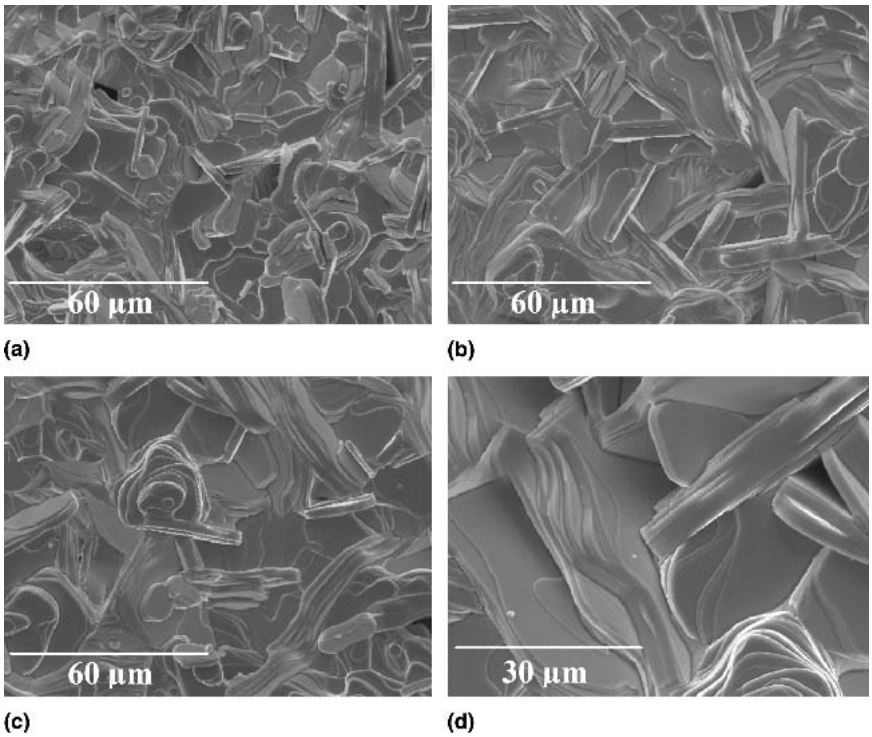

FIG 2. SEM micrographs of pellets sintered for (a) 12 h, (b) 25 h, and (c, d) 50 h; $Bi_{2.5}Ca_{2.5}Co_2O_x$ starting composition.

explained by a larger content of Bi_2O_3 phase, which melts at 817 °C and probably generates a larger amount of liquid phase during the sintering. Consequently, element diffusion and growth kinetics are improved. Although the phase equilibrium in our system is still unclear, and the growth mechanism not solved, the rounded shape of the growth front [Fig. 2(d)] and the drastic increase of the grain size versus the sintering time tend to indicate the presence of a liquid phase during high-temperature processing.

Secondary phase particles, with pseudo-square polyhedral shapes, were clearly observed for samples with the $Bi_{1.8}Ca_2Co_2O_x$ composition [Fig. 1(d)]. The specific shape of these particles correlated by EDS microanalysis identifies these grains as Co_3O_4. This observation directly correlates to the cationic ratio of the platelike grains (Table I) in samples prepared from $Bi_{1.8}Ca_2Co_2O_x$ and $Bi_{2.5}Ca_{2.5}Co_2O_x$ starting compositions sintered for 50 h. Indeed, EDS measurements, performed on 8 grains, revealed the $Bi_{2.5}Ca_{2.5}Co_2O_x$ phase tends to be preferentially stabilized at 850 °C in both compositions. The presence of Co_3O_4 phase, in excess in the samples with the initial $Bi_{1.8}Ca_2Co_2O_x$ composition, is then consistent with microprobe analysis. The absence of secondary phases, observable in Fig. 2, is another indication that the cationic ratio of the Bi–Ca–Co–O system, usually notated as $Bi_2Ca_2Co_2O_x$, should be represented, in the framework of this study, by $Bi_{2.5}Ca_{2.5}Co_2O_x$. This composition is also similar to the single crystal composition reported by Tarascon et al.[11]

It is also clear from the XRD powder pattern shown in Fig. 3, which is almost identical to those of all samples, that the powders correspond to the Bi–Ca–Co–O system,[7,11,12] even if an accurate comparison is not possible due to the different compositions in the cited papers and the absence of crystallographic models for our phase composition. The Co_3O_4 phase was not detected by x-ray diffraction when $Bi_{1.8}Ca_2Co_2O_x$ was used as a starting material, probably due to its relative small amount, the higher crystallinity of the $Bi_{2.5}Ca_{2.5}Co_2O_x$ phase, and some fluorescence.

Figure 4 shows typical TG/DTA curves of sintered $Bi_{1.8}Ca_2Co_2O_x$ powders. Variations were not observed between the different samples, even though we expected

TABLE I. EDS analyses performed on platelike grains of $Bi_{1.8}Ca_2Co_2O_x$ and $Bi_{2.5}Ca_{2.5}Co_2O_x$ pellets sintered for 50 h at 850 °C.

	$Bi_{1.8}Ca_2Co_2O_x$			$Bi_{2.5}Ca_{2.5}Co_2O_x$		
Grain No.	Bi	Ca	Co	Bi	Ca	Co
1	2.405	2.284	2	2.451	2.399	2
2	2.369	2.388	2	2.634	2.613	2
3	2.456	2.44	2	2.263	2.197	2
4	2.297	2.371	2	2.754	2.748	2
5	2.511	2.426	2	2.468	2.469	2
6	2.385	2.504	2	2.497	2.535	2
7	2.447	2.42	2	2.376	2.32	2
8	2.512	2.417	2	2.628	2.541	2
Average	2.423	2.406	2	2.509	2.477	2

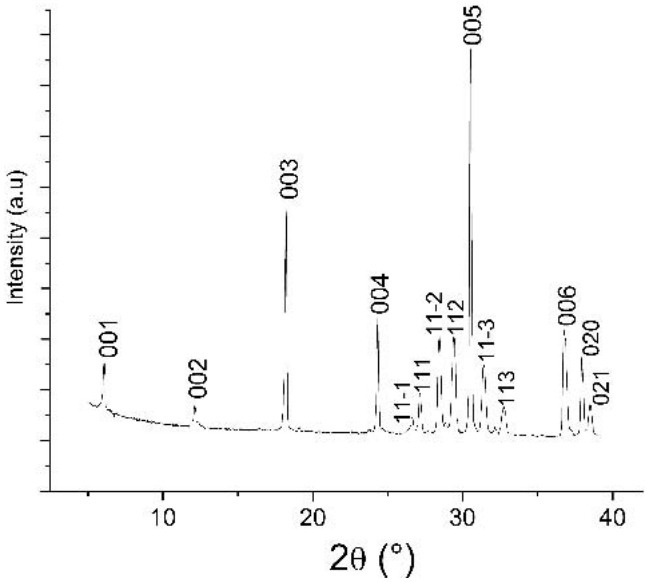

FIG 3. XRD powder pattern of sintered pellets; $Bi_{1.8}Ca_2Co_2O_x$ starting composition.

to observe the dissociation reaction $Co_3O_4 \rightarrow 3CoO + 1/2O_2$ at 900 °C in the samples with the $Bi_{1.8}Ca_2Co_2O_x$ composition. The related endothermic peak of this dissociation is probably superposed with the stronger endothermic peak at 945 °C, associated with a 2.5% weight loss, and corresponding to the decomposition of the $Bi_{2.5}Ca_{2.5}Co_2O_x$ phase. The last broad peak highlights the melting of the phase at around 1000 °C, as it has been confirmed by quench experiments, whereas the small endothermic peaks at 780 °C and 825 °C (indicated by arrows) tend to confirm our hypothesis concerning the presence of liquid phase during the sintering. The origins are not still elucidated but we can emphasize a preliminary reaction with the Bi_2O_3 phase melted at high temperature during the sintering step. Figure 5 shows the

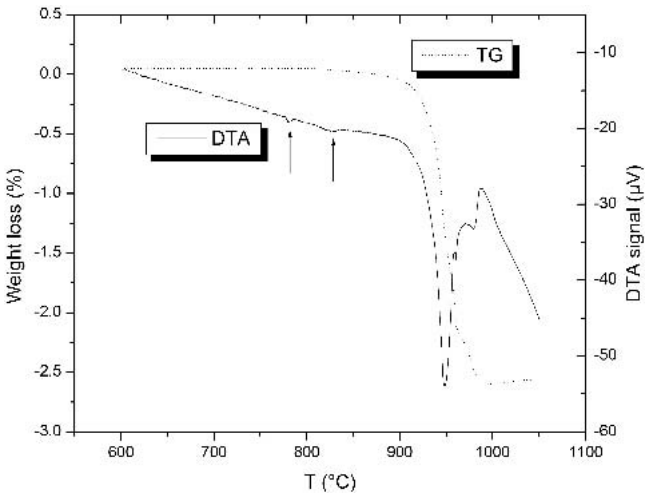

FIG. 4. TG/DTA curves of sintered powders; $Bi_{1.8}Ca_2Co_2O_x$ starting composition.

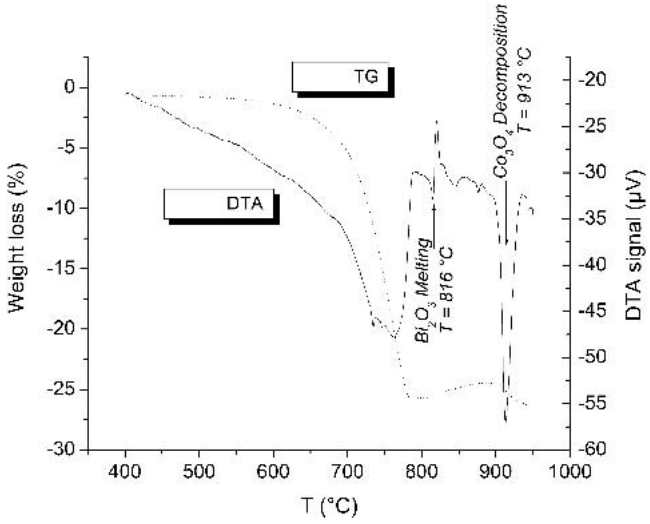

FIG. 5. TG/DTA curves of unreacted powder; $Bi_{1.8}Ca_2Co_2O_x$ starting composition.

TG/DTA curve of unreacted $Bi_{1.8}Ca_2Co_2O_x$ powder (before sintering) composed of Bi_2O_3, $CaCO_3$, and Co_3O_4 precursor powders. The first broad endothermic peak is evidence of decarbonation of the precursor $CaCO_3$ phase, followed by the melting of the Bi_2O_3 phase at 816 °C. The subsequent exothermic peak tends to indicate the reaction of the liquid phase to promote the phase formation. The two small endothermic peaks at 845 and 876 °C have not been indexed, whereas the dissociation reaction of the Co_3O_4 phase at 900 °C is clearly observed with a maximum peak intensity at 916 °C. A more in-depth study is now underway to clarify the partial melting reaction occurring at high temperature in this Bi–Ca–Co–O system and the composition of the liquid phase. According to the phase diagram of Bi_2O_3-CaO system by Lurton et al.,[13] many phases near the Bi-rich compositions can be stabilized at high temperatures, and the origin of the partial melting must be studied in depth.

Because the synthesis of almost pure $Bi_{2.5}Ca_{2.5}Co_2O_x$ phase is well controlled, the texturation of bulk materials by the hot-forging technique was investigated. The liquid phase reaction here represents an interesting aspect as a promoter of efficient stacking and sliding of such large platelike grains during the thermomechanical processing. According to our experience in the field of superconducting Bi2223 materials,[14] where partial melting reaction occurs at high temperatures,[15] the similar plastic deformation we observed here on $Bi_{2.5}Ca_{2.5}Co_2O_x$ cobaltites suggests a partial melting reaction. On the other hand, the reduction in the number of grain boundaries combined with efficient (00*l*) texture development may improve TE performance. Due to the strong electrically resistive behavior of the Co_3O_4 phase, only powders resulting from pellets of the $Bi_{2.5}Ca_{2.5}Co_2O_x$ composition sintered for 12, 25, and 50 h were used for hot-pressing experiments.

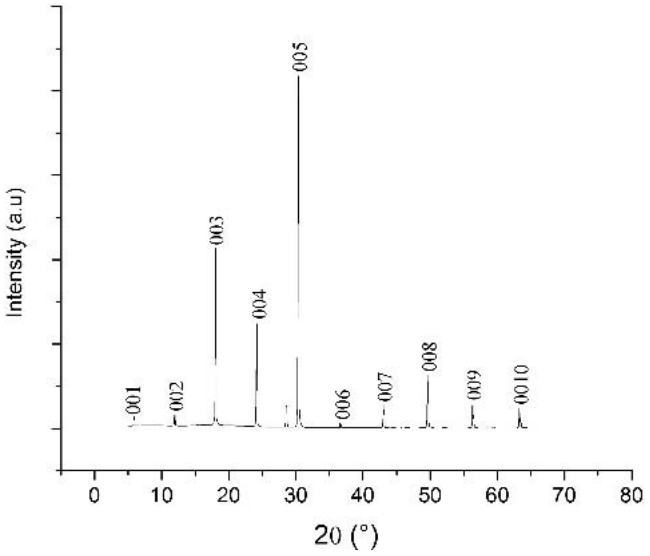

FIG. 6. XRD pattern of the textured specimen composed of powder sintered for 50 h.

These powders, as evidenced by the SEM microstructures (Fig. 2), present a different grain size distribution with average grain size increasing with increasing sintering time. XRD patterns for the polished surface perpendicular to the hot-forging direction of the three textured materials exhibit mainly (00*l*) diffracted peaks as a sign of the strong preferential orientation (Fig. 6). Thermomechanical treatment is thus highly effective for the development of (00*l*) texture. However, the question of the quantitative aspect of texture versus grain size remains open. Consequently, we extracted the DD_{max} quantitative texture parameter to estimate the degree of alignment of the specimens; both the surface and the core (after polishing to a depth of 1 mm) were analyzed. As can be seen in Table II, the degree of orientation of the surface is higher than that in the core. The orientation distribution densities calculated for the sample surface reach values around 8 times larger than those in the core. The pole figures shown in Fig. 7 clearly highlight the difference in texture strength with a much sharper *c* axis in the surface analysis. This phenomenon is of course related to mechanical pressure applied during hot-forging, which promotes an efficient sliding and stacking of grains at the surface. The surface is then highly aligned (DD_{max} >

TABLE II. Maximum of the distribution density for textured materials initially composed of (a) 12 h, (b) 25 h, and (c) 50 h sintered powders; surface and core analyses.

	DD_{max} (m.r.d.)	
Samples	Surface	Core
12 h	132	21.9
25 h	161	23.2
50 h	180	22.8

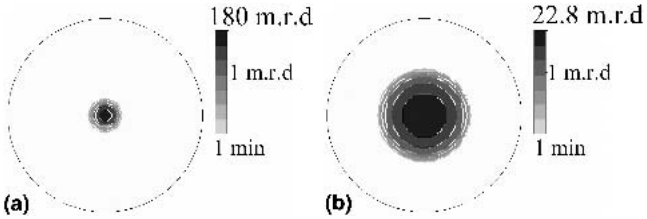

FIG. 7. {005} pole figures calculated for (a) the surface and (b) the core of the textured specimen prepared from powder sintered for 50 h.

140 m.r.d.) compared to the core (DD_{max} ~ 22 m.r.d.). In addition, the degree of orientation on the sample surface is improved with larger grain size powder, whereas the core presents almost the same texture strength. This result can be explained by the larger surfaces of the platelike grains, which are probably easier to align on the surface than in the core during the first cold-pressing but also during the hot-forging process. Figures 8(a) and 8(b)

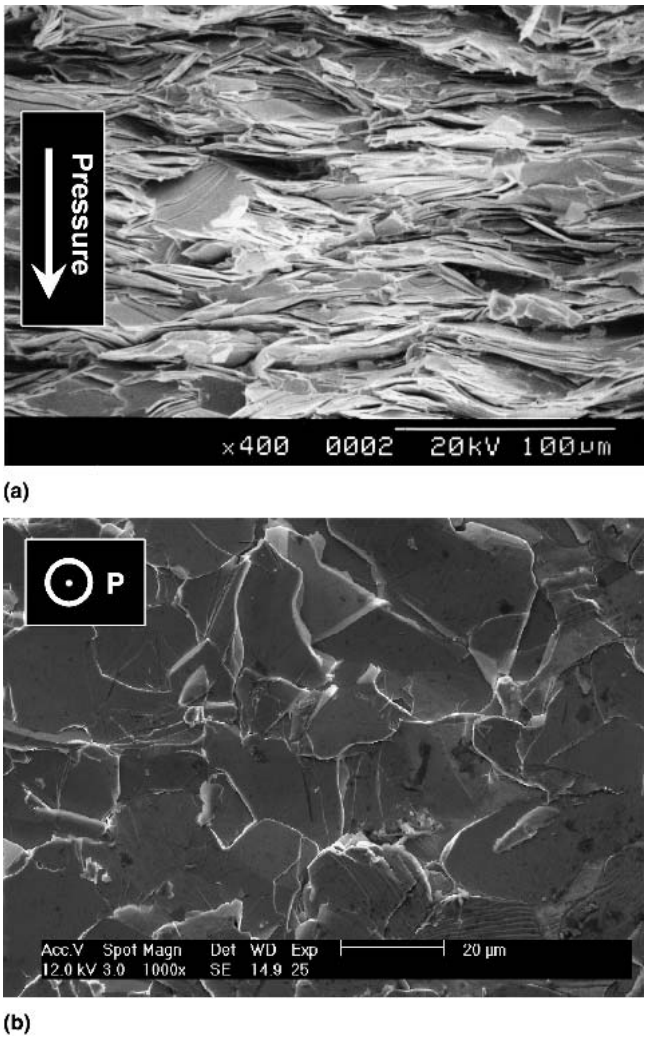

FIG. 8. SEM photograph of a fracture surface parallel to the pressure direction. The textured specimen was initially composed of 50 h sintered powder.

show, respectively, the typical core transverse section and the sample surface where one can appreciate the alignment of the large platelike grains perpendicular to the pressure direction.

Figure 9 shows the temperature dependence of (a) ρ values and (b) *S* values measured along the direction perpendicular to the hot-forging pressure direction. The ρ values are significantly reduced for powders synthesized with longer sintering times. The texture improvement on the surface could be one reason for the decrease in ρ_{ab} in our ceramic samples. The enhancement of texture would increase the contribution of the conduction path along the *ab* plane with low ρ values and decrease the same along the *c* axis with high ρ. However, the well-oriented surface represents only a few percentage of the entire volume of a sample. In consequence, it can be

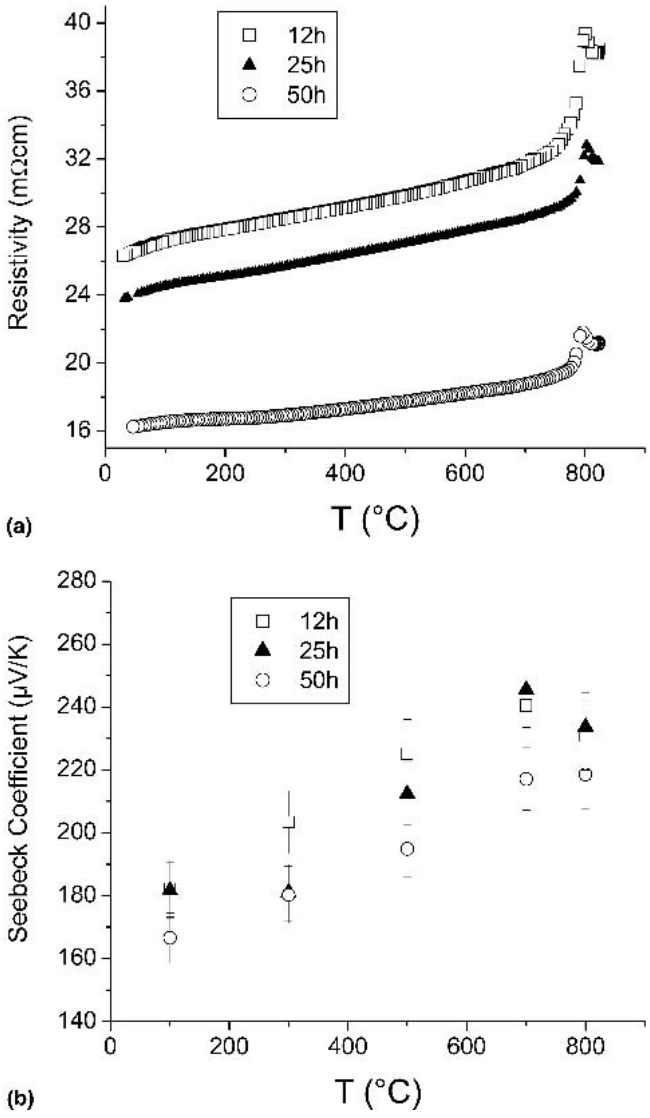

FIG. 9. (a) Electrical resistivity and (b) Seebeck coefficient versus temperature curves. Textured specimens initially composed of 12 h, 25 h, and 50 h sintered powders.

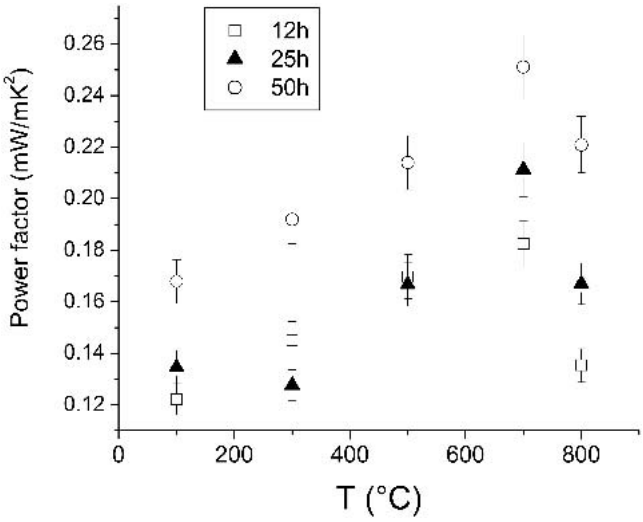

FIG 10. Power factor versus temperature curve; textured specimens were initially composed of 12 h, 25 h, and 50 h sintered powders.

emphasized that the larger grain-size powders, obtained at longer sintering times, circumvent the detrimental effect of grain boundaries on the transport properties. The scattering of carriers due to the disordered atom layers at the grain boundary is limited by larger platelike grains and a lower density of grain boundaries in the material.

On the other hand, the jump in resistivity observed at temperatures over 770 °C is consistent with our hypothesis on the presence of a liquid phase at high temperature. This reversible effect tends to indicate a partial melting reaction. Investigations are underway to clarify the reaction mechanism. As *S* values among the three samples remain virtually unchanged over the entire temperature range, in the case of the sample synthesized from powder sintered for 50 h, the resulting power factor is increased and reaches 0.25 mW/mK^2 at 700 °C (Fig. 10). According to the results reported in the literature, this material presents the most interesting properties in the Bi–M–Co–O system (with M = Ca, Sr, Ba). However, the decrease of *S* values at around 800 °C and the drastic increase of electrical resistivity, probably due to the liquid phase reaction, cause the power factor to lessen significantly. This observation is important from the viewpoint of applications for which the use of this Bi–Ca–Co–O material would be limited to temperatures under 770 °C.

IV. CONCLUSIONS

Large platelike grains of the $Bi_{2.5}Ca_{2.5}Co_2O_x$ phase were synthesized. To improve the TE properties, *c*-axis-oriented materials were successfully fabricated by the hot-forging method. High texture strengths were obtained and resulted in power factor of ~0.25 mW/mK^2 at 700 °C. The downside of this material remains the drastic

increase of electrical resistivity due to a liquid phase reaction at high temperature, which limits it to applications under 770 °C.

ACKNOWLEDGMENT

The authors are grateful to Dr. Catherine Henrist for fruitful discussions and valuable comments.

REFERENCES

1. I. Terasaki, Y. Sasago, and K. Uchinokura: Large thermoelectric power in $NaCo_2O_4$ single crystals. *Phys. Rev. B* **56,** R12685 (1997).
2. S. Li, R. Funahashi, I. Matsubara, K. Ueno, and H. Yamada: High temperature thermoelectric properties of oxide $Ca_9Co_{12}O_{28}$. *J. Mater. Chem.* **9,** 1659 (1999).
3. A.C. Masset, C. Michel, A. Maignan, M. Hervieu, O. Toulemonde, F. Studer, B. Raveau, and J. Hejtmanek: Misfit-layered cobaltite with an anisotropic giant magnetoresistance: $Ca_3Co_4O_9$. *Phys. Rev. B* **62,** 166 (2000).
4. R. Funahashi, I. Matsubara, H. Ikuta, T. Takeuchi, U. Mizutani, and S. Sodeoka: An oxide single crystal with high thermoelectric performance in air. *Jpn. J. Appl. Phys.* **39,** L1127 (2000).
5. R. Funahashi, I. Matsubara, and S. Sodeoka: Thermoelectric properties of $Bi_2Sr_2Co_2O_x$ polycrystalline materials. *Appl. Phys. Lett.* **76,** 2385 (2000).
6. A. Maignan, S. Hébert, M. Hervieu, C. Michel, D. Pelloquin, and D. Khomskii: Magnetoresistance and magnetothermopower properties of Bi/Ca/Co/O and Bi(Pb)/Ca/Co/O misfit layer cobaltites. *J. Phys. Condens. Matter* **15,** 2711 (2003).
7. H. Itahara, C. Xia, J. Sugiyama, and T. Tani: Fabrication of textured thermoelectric layered cobaltites with various rock salt-type layers by using β–$Co(OH)_2$ platelets as reactive templates. *J. Mater. Chem.* **14,** 61 (2004).
8. E. Guilmeau, D. Chateigner, and J.G. Noudem: Sinter-forging of strongly textured Bi2223 discs with large J_cs: nucleation and growth of Bi2223 from Bi2212 crystallites. *Supercond. Sci. Technol.* **15,** 1436 (2002).
9. E. Guilmeau, R. Funahashi, M. Mikami, K. Chong, and D. Chateigner: Thermoelectric properties–texture relationship in highly oriented $Ca_3Co_4O_9$ composites. *Appl. Phys. Lett.* **85,** 1490 (2004).
10. M. Mikami, R. Funahashi, M. Yoshimura, Y. Mori, and T. Sasaki: High-temperature thermoelectric properties of single-crystal $Ca_3Co_2O_6$. *J. Appl. Phys.* **94,** 6579 (2003).
11. J-M. Tarascon, R. Ramesh, P. Barboux, M.S. Hedge, G.W. Hull, L.H. Greene, M. Giroud, Y. LePage, W.R. McKinnon, J.V. Waszcak, and L.F. Schneemeyer: New non-superconducting layered Bi-oxide phases of formula $Bi_2M_3Co_2O_y$ containing Co instead of Cu. *Solid State Commun.* **71,** 663 (1989).
12. M. Hervieu, Ph. Boullay, C. Michel, A. Maignan, and B. Raveau: A new family of misfit layered oxides with double rock salt layers $Bi_\alpha(A_{0.75\pm\varepsilon}Bi_{0.25\pm\varepsilon}O)_{(3+3x)/2}MO_2$($A$ = Ca, Sr and M = Co, Cr). *J. Solid State Chem.* **142,** 305 (1999).
13. B.P. Burton, C.J. Rawn, R.S. Roth, and N.M. Hwang: Phase equilibria and crystal chemistry in portions of the system SrO–CaO–Bi_2O_3–CuO, Part IV—The system CaO–Bi_2O_3–CuO. *J. Res. Natl. Inst. Stand. Technol.* **98,** 469 (1993).
14. E. Guilmeau, D. Chateigner, and J.G. Noudem: Effect of the precursor powders on the final properties of hot-forged Bi2223 textured discs. *Supercond. Sci. Technol.* **16,** 484 (2003).
15. P. Morgan, J.D. Piche, and R.M. Housley: Use of a thermal gradient to study the role of liquid phase during the formation of bismuth high temperature superconductors. *Physica C* **191,** 179 (1992).